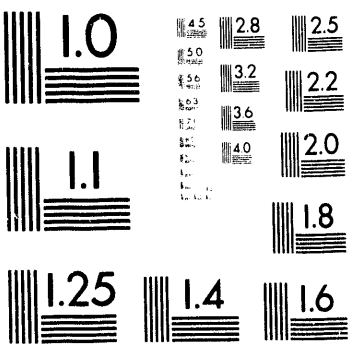
1.0
1.1
1.25
1.4
1.6
1.8
2.0
2.2
2.5
2.8
3.2
3.6
4.0
4.5
5.0
5.6
6.3
7.1

1 of 1

# The Effect of Microstructural Evolution on Superplasticity in $Ni_3Si(V,Mo)$

S. L. Stoner and A. K. Mukherjee

This paper was prepared for submittal to the
Advances in Superplasticity and Superplastic Forming
Chicago, IL
November 1-5, 1992

October 1992

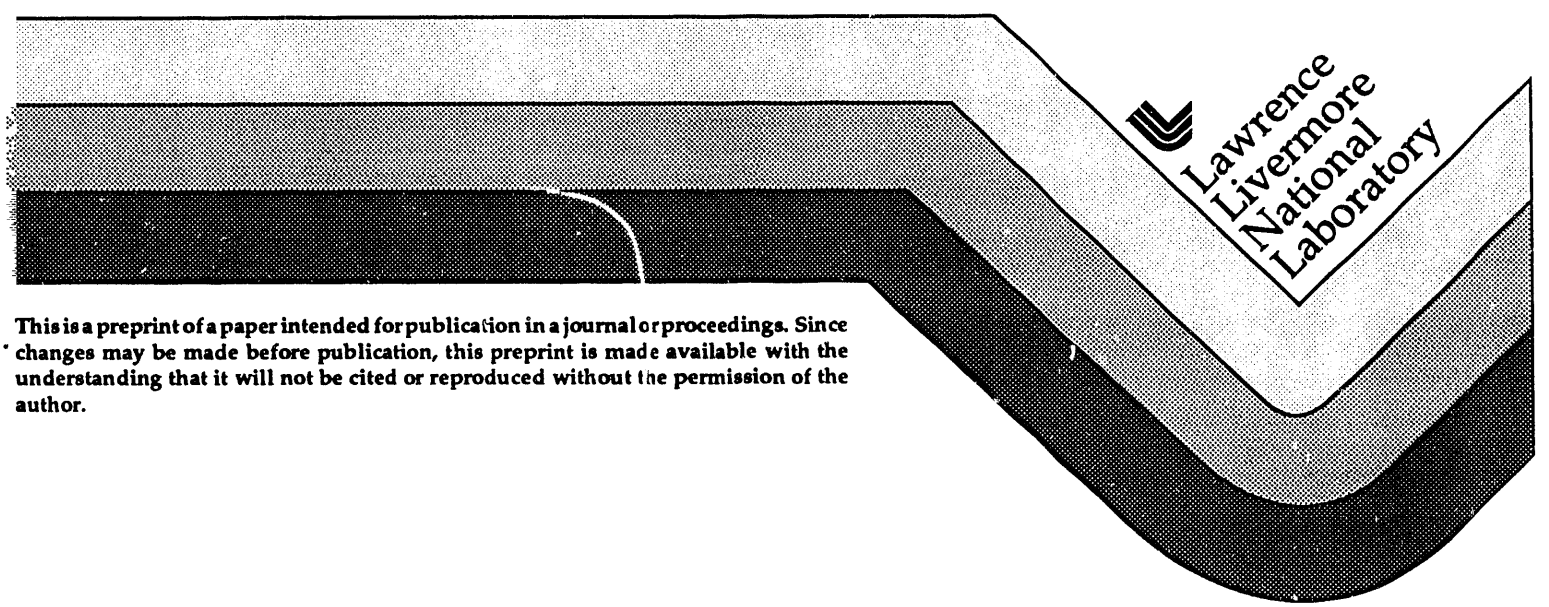

# THE EFFECT OF MICROSTRUCTURAL EVOLUTION ON SUPERPLASTICITY IN $Ni_3Si(V,Mo)$

Susan L. Stoner+ and Amiya K. Mukherjee*

+Lawrence Livermore National Laboratory, University of California, Livermore, California

*Department of Mechanical, Aeronautical and Materials Engineering, University of California, Davis, California

## Abstract

To further the understanding of superplasticity in intermetallics, this paper presents results of experimental investigations on an intermetallic alloy based on nickel silicide. Specifically, the evolution of the microstructure and its influence on superplastic performance is discussed. In the duplex microstructure, one phase showed grain growth, and the other, grain refinement. Cavitation occurred at interphase boundaries and final failure was by interlinkage of these cavities. Annealing the material improved the homogeneity of the microstructure. The annealed material showed improved strain rate sensitivity values and enhanced superplasticity. Microstructural features and ductility were also influenced by changing the orientation of the tensile axis. Though a transverse orientation showed more cavitation than longitudinal, it yielded greater elongation. An increased resistance to cavity coalescence in the transverse direction played a role in the enhanced ductility.

## Introduction

Intermetallic alloys possess many attractive mechanical properties. Because of their ordered nature, dislocation motion is limited, particularly at elevated temperatures, resulting in exceptional high temperature strength. The density of many intermetallics is quite low, especially those based on the lighter elements like $Ti_3Al$. Because of their ability to form protective oxide films, intermetallics such as silicides and aluminides are highly resistant to oxidation and corrosion.

In spite of these attributes, interest in the use of intermetallics has been limited in the past because these materials show limited ductility. The inherent brittleness of intermetallics arises from the limited number of slip systems in their ordered crystal structure and a propensity for grain boundary embrittlement. In recent years, however, major advances have been made in improving the ductility of these materials. Through alloying and control of the microstructure with thermomechanical processing, it has been shown that the ductility of several intermetallic systems can be substantially improved (1-5). With progress such as this, intermetallic alloys are promising candidates for use in advanced aerospace, turbine engine, and power plant designs.

Superplasticity has been shown in a number of intermetallic alloys. In order to develop and optimize the superplastic forming capabilities of these materials, their microstructural features and mechanical properties must be well characterized. The effect of variables such as thermomechanical processing and test or forming parameters on the superplastic performance must be understood as well.

This work considers an intermetallic alloy based on nickel silicide, $Ni_3Si(V,Mo)$. This alloy shows superplasticity at temperatures from 1273 - 1383 K (6) and at strain-rates from $10^{-4}$ to 1 $s^{-1}$ (6,7). This paper focuses on the characteristics of the microstructure and its correlation to the superplastic behavior the $Ni_3Si$ alloy.

## Experimental Details

The composition of the material used for this study was (wt%) Ni-9Si-3.1V-4Mo. Vanadium and the molybdenum were added to the binary $Ni_3Si$ to promote superplasticity by stabilizing the b phase in the duplex microstructure.

A 1 in. x 1 in. x 5 in. ingot was produced by arc melting and drop casting of pure metal constituents. The thermomechanical processing of the material included a homogenization anneal, hot forging to a thickness of 0.6 in., hot rolling to a thickness of 0.1 in., and a final anneal at 1223 K for 16 hours. The final anneal was designed to restore maximum room temperature ductility.

Tensile specimens were cut from the material by electrical discharge machining. Specimens were prepared primarily with the tensile axis parallel to the rolling direction. (Unless otherwise stated, the results presented in this paper were obtained from specimens prepared in this orientation.) The final gage dimensions were 0.225 in. x 0.375 in. x 0.080 in. The specimens were tested using a digital controlled Instron 4505 tensile machine, interfaced with a data acquisition system. Tests were performed in an argon atmosphere surrounded by a radiant heat furnace.

The material was examined using optical metallography, scanning electron microscopy, and transmission electron microscopy. Cavitation was studied using a Ziess image analysis system.

A Quantimet image analyzer was used to obtain grain areas using a minimum of 250 grains for each measurement. The following equation given by ASTM E112, was used to convert grain area to a linear intercept value.

$$\text{Linear intercept} = .886(\text{grain area})^{0.5} \quad (1)$$

Grain sizes are expressed as the linear intercept value measured in the plane normal to the sample thickness.

## Results and Discussion

The microstructure of the $Ni_3Si(V,Mo)$, as-received, is shown in Figure 1. The material has a duplex microstructure with a third phase present as precipitates. A large distribution of grain sizes and texturing in the direction of rolling is observed. Strings and large groups of grains of a single phase are apparent.

The smooth, dark grains are $L1_2$ cubic beta ($\beta$) phase. The average size of the $\beta$ grains is 3.8 mm. The textured, light grains consist of a phase mixture of alpha ($\alpha$) - Ni solid solution phase and cubic $\beta$ phase dispersions. This phase mixture will be referred to as ($\alpha$+$\beta$) from here on. The average size of the ($\alpha$+$\beta$) grains is 11.9 $\mu$m. The third phase is Mo-rich precipitates, 1 - 2 $\mu$m in diameter, which are randomly distributed throughout the microstructure. There is no apparent change in the size or volume fraction of these precipitates with deformation, suggesting they are insignificant to superplasticity in the $Ni_3Si$ alloy.

### Microstructural evolution

Strain-enhanced growth of the $\beta$ grains and strain-enhanced refinement of the ($\alpha$+$\beta$) phase grains occurs during superplasticity. Hence, the two phases become more equal in size with strain. This is demonstrated clearly in the micrographs in Figure 2. The microstructure at the grip is shown compared with that near the tip for a specimen that was tested at 1343 K and a strain-rate ($\varepsilon$) of $10^{-3}$ $s^{-1}$ (the direction of rolling is shown). These micrographs were made using back scattered electrons. The textured, multi-colored grains are the ($\alpha$+$\beta$) phase. The singe-colored grains are $\beta$ phase and the white spots are the Mo-rich precipitates. It is also evident that grains that are initially elongated become more equiaxed with strain. These observations are consistent with the general tendency for the microstructure of superplastic materials to become more uniform with deformation.

True stress/true strain curves are shown in Figure 3 for constant strain-rates tests conducted at 1343 K and at strain-rates of: $6x10^{-4}$ $s^{-1}$, $1x10^{-3}$ $s^{-1}$, and $8x10^{-2}$ $s^{-1}$. Tensile stability is clearly demonstrated at the lower two strain rates. (Flow stress and strain-rate sensitivity as a function of temperature and strain-rate have been presented elsewhere (8)).

The strain-hardening demonstrated at the lower two strain-rates is related to the dynamic grain growth in the $\beta$ phase. Figure 4 shows $\beta$ grain growth as a function of local strain (expressed as a reduction in area) for the three strain-rates shown in Figure 3. Dynamic grain growth was determined from the difference between the grain size in the gage and in the grip.

Growth of the β phase increases with decreasing strain-rate. The lack of grain growth at the highest strain-rate is consistent with the studies of Wilkinson and Caceras (9). In a number of superplastic materials, they showed a tendency for the grain growth rate to reach a plateau at high strain rates. This results because grain boundary migration is a time-dependent process and is therefore limited at high strain-rates.

Hamilton (10) has suggested that strain hardening is necessary for tensile stability and hence improves superplasticity. This is consistent with the results that have been presented. With decreasing strain-rate, both an increase in tensile stability and an increase in grain growth are shown.

Refinement in the (α+β) phase was observed in all tests and appeared to be maximum at the lowest strain-rate. The mechanism of the refinement in the (α+β) phase is uncertain at this time. No signs of recrystallization were shown. However, since the lowest strain-rate showed the best superplastic behavior, it appears that the maximum in grain refinement might be linked to a maximum in grain boundary sliding. Since long range cooperative grain boundary sliding brings about a redistribution of the phase structure, it might be that the (α+β) phase is broken up in this process. Cooperative sliding has been discussed by several authors (11,12,13) and Yang, et.al., (13) associated the breaking up of the $\alpha_2$ phase in $Ti_3Al$ alloys to this behavior.

Cavitation was observed in the $Ni_3Si$ alloy during superplasticity. Cavities are located almost exclusively at β /(α+β) interfaces. For a given strain, an increase in cavitation with decreasing strain-rate was observed. The final specimen failure in all tests occurred by the interlinkage of cavities.

Effect of test orientation and microstructural anisotropy

It is clear from Figure 1 that grains are elongated in the direction of rolling in the as-received material. All of the results discussed thus far have considered testing with the tensile axis parallel to this direction. To assess the effect of microstructural anisotropy on the superplasticity of $Ni_3Si(V,Mo)$, specimens were additionally prepared with their axes parallel to the transverse direction.

Figure 5 compares the stress/strain behaviors for loading in the longitudinal and transverse directions. These tests were conducted at a constant strain-rate of $10^{-3}$ $s^{-1}$ at 1343 K. The specimen tested in the transverse direction achieved greater terminal ductility while reaching a higher maximum stress.

Strain-rate sensitivity (m) curves for the two orientations were generated. The total strain (ε) achieved in the tests used to make these curve was low ($\varepsilon < 0.4$). For strain-rates ranging from $10^{-4}$ to $10^{-1}$ $s^{-1}$, the m values for the two orientations were approximately the same. Thus, it appears that the enhanced ductility in the transverse direction cannot be attributed to a better strain-rate sensitivity. The discrepancy may lie in the assumption that the calculated values of m are not sensitive to the structural details that vary with strain. At strains less than 0.4, where the m curves were generated, the longitudinal and transverse curves in Figure 5 are similar. However, at a higher level of strain the two begin to differ significantly. It might be that at higher strains, the strain-rate sensitivity in the longitudinal orientation falls off at a lower strain than that for the transverse orientation. Since the instability parameter is defined by the strain hardening coefficient as well as the strain-rate sensitivity, a

difference in this value for the two orientations may also play a role in the relative behaviors.

The growth of the β phase and refinement of the (α+β) phase were similar in the two specimens. The cavitation characteristics for the two however were quite different. These characteristics might be different enough to influence the relative true strain-rate sensitivity values and/or the strain hardening coefficients. Numerous long cavity strings, primarily in the direction of the tensile axis, were present in the longitudinal specimen. Cavities nucleated at β /(α+β) interphases and tended to coalesce along the grain boundaries that were elongated in the direction of loading. Crack-like growth of cavities was observed as well.

The transverse specimen showed a greater resistance to cavity coalescence than the longitudinal specimen. Some cavity strings were observed but they were shorter and far less numerous than in the longitudinal specimen. Crack-like growth was absent. Some coalescence of cavities into large holes was seen in the transverse specimen. It is interesting as well that the transverse orientation showed more cavitation, particularly at low and intermediate strains, than the longitudinal orientation. For specimens tested in both directions, the final failure occurred by cavity interlinkage. This is shown clearly in Figure 6 by the substantial cross sectional area and lack of extensive necking at the fracture tip of a specimen that achieved 387% elongation.

From the observations discussed above, the following explanation of the relative behaviors shown in Figure 5 is proposed. At lower strains, the stress/strain behavior of the two orientations are similar as reflected by their comparable strain-rate sensitivities. At a true strain of approximately 0.8, the coalescence of cavities has become sufficient in the longitudinal orientation to initiate necking and the curve begins to drop off. Because of a greater resistance to cavity interlinkage in the transverse direction, the strain hardening behavior continues and initiation of necking is delayed to a higher strain. This results in a higher maximum flow stress and a larger terminal ductility in the transverse direction.

Effect of annealing

As discussed earlier, the as-received $Ni_3Si(V,Mo)$ microstructure shows considerable anisotropy. It is well established that ideal superplastic microstructures contain fine, uniform grains. This suggests that improvement in the initial microstructure of the $Ni_3Si$ alloy through thermomechanical processing might lead to improvement in superplastic performance.

The as-received material was annealed for four hours at 1323K in a vacuum furnace. (From here on "annealed" will refer to this particular anneal.) The grain size distributions in the β and (α+β) phases resulting from the anneal are compared to those in the as-received microstructure in Figure 7. The distributions in both phases in the annealed condition are narrower than those in the as-received condition. In the β phase, a shift towards larger sizes is apparent, owing to static grain growth. The resulting average size of the β grains in the annealed material is 5.0 μm. That of the (α+β) grains remained at 11.9 μm. This latter result indicates that deformation is necessary to induce (α+β) refinement in $Ni_3Si(V,Mo)$.

The grains in both phases are more equiaxed in the annealed material. Additionally, the two phases are more randomly distributed following the anneal, i.e., there are not

as many strings or groups of grains of a single phase. Mechanical twins which are present in the as-received microstructure are not as numerous in the annealed microstructure.

The stress/strain behavior of the $Ni_3Si$ alloy is compared for the as-received and the annealed conditions in Figure 8. More strain was achieved in the annealed material. This is an expected result since all of the changes in the microstructure due to the anneal tend to be favorable for superplasticity.

Figure 9 compares the strain-rate sensitivities for the as-received and annealed conditions. The strain-rate sensitivity for the annealed material was higher than that of the as-received material over a wide range of strain-rates. At the highest rates, where the m values are equal for the two conditions, deformation is no longer governed by superplasticity. Assuming the strain-rate sensitivities for the two conditions show the same trend with increasing strain, these curves are consistent with the stress/strain behaviors shown in Figure 8.

A greater amount of strain hardening is observed in the annealed material. The amount of strain-enhanced growth of the $\beta$ grains in the as-received and annealed materials was approximately the same. However , because the initial size of the $\beta$ phase grains was larger in the annealed material, this may at least partially explain why more hardening is shown in the annealed material.

In addition to grain size and uniformity of the phases, it is likely that there is other factors contributing to the enhanced ductility observed in the annealed material. One such factor might be the structure of the grain boundaries. It is known that the mechanical behavior of metals and alloys is influenced by grain boundary structure as well as grain boundary area.

In the intermetallic TiAl, Imayev and coworkers (14) showed that superplastic performance was deteriorated by the presence of twin boundaries. In contrast to "random" boundaries, grain boundary sliding is impeded by twin boundaries which trap lattice dislocations, even at high temperatures. Using thermomechanical processing, Imayev, et.al., varied the proportionate number of random boundaries to twin boundaries in TiAl samples. For those with a higher percentage of the random type, better strain-rate sensitivity values and greater superplastic elongations were shown. For the $Ni_3Si(V,Mo)$, it might be that annealing the material reduced the number of twin or other types of "special" boundaries, which impede grain boundary sliding, in the microstructure. The annealed microstructure could then have a larger percentage of "random" boundaries than the as-received microstructure, which better facilitate superplasticity.

The cavitation was measured in the tested as-received and annealed specimens. At higher levels of strain, the two showed approximately the same amount of cavitation and cavity coalescence. At low strains however, the annealed specimen showed less cavitation, owing most likely to the more uniform starting structure.

## Conclusions

Results of experimental investigations related to microstructural evolution in super stic $Ni_3Si(V,Mo)$ have been presented. The microstructure plays a significant role in the superplastic behavior of this material.

At the lower strain-rates tested, strain-enhanced growth occurred in the β phase grains during superplastic deformation. The stress/strain curves show strain hardening as a result of grain growth. At the highest strain-rate, β grain growth was absent and the stress/strain curve showed no tensile stability. Refinement was observed in the (α+β) grains at all strain-rates tested.

The orientation of the test with respect to the microstructure had a significant effect on the superplastic behavior of this alloy. For tension in the transverse direction, more total strain was achieved and more strain hardening was observed than for tension in the longitudinal direction. The improved superplasticity is attributed to a greater resistance to cavity interlinkage in the transverse direction.

Annealing the material resulted in a more uniform starting microstructure. The annealed microstructure showed improved strain-rate sensitivity values and a greater total elongation than the as-received microstructure. The structure of the grain boundaries might play a role in the enhanced superplasticity seen in the annealed microstructure.

## References


1. K. H. Hahn and K. Vedula, Scripta Metall., 23, (1979),7.

2. C.T. Liu, C.L. White, C.C. Koch, and E.H. Lee, in High Temperature Materials Chemistry II, Vol. 83-7, edited by Munir Cubicciotti , The Electrochem. Soc. Inc., (1983), 32.

3. K. Aoki and O. Izumi, Nippon Kinzoku Gakkaishi, 43, (1979), 1190.

4. M.J. Blackburn and M.P. Smith, Air Force Technical Report, AFWAL-TR-81-4046 (1981).

5. J. Wadsworth and F.H. Froes, J. Metals, 41, (1989), 12.

6. T.G. Nieh, in Superplasticity in Metals, Ceramics, and Intermetallics, edited by M.J. Mayo, M. Kobayashi and J. Wadsworth, MRS, Pittsburgh, PA, (1990), 189.

7. S.L. Stoner, "Superplasticity in a Nickel Silicide Alloy, $Ni_3Si(V,Mo)$" (Masters thesis, University of California at Davis, 1984).

8. S.L. Stoner and A.K. Mukherjee, Materials Science and Engineering, A153 , (1992), 465.

9. D.S. Wilkinson and C.H. Caceres, Acta Metall., 32, (1984),415.

10. C.H. Hamilton, in Strength of Metals and Alloys, edited by H.J. McQueen, J.P. Bailon, and J.I. Dichson, Pergamon, Oxford, (1986), 831.

11. M.G. Zelin and M.V. Alexsandrova, in Superplasticity in Advanced Materials, edited by S. Hori, M. Tokizane, and N. Furushiro, Japan Society for Research on Superplasticity, Osaka Japan, (1991), 63.

12. R.Z. Valiev and M.G. Zelin, in Superplasticity in Advanced Materials, edited by S. Hori, M. Tokizane, and N. Furushiro, Japan Society for Research on Superplasticity, Osaka Japan, (1991), 95.

13. H.S. Yang, M.G. Zelin, R.Z. Valiev, and A.K. Mukherjee, Scripta Metall., 26, (1992), 1707.

14. R.M. Imayev, O.A. Kaibyshev, and G.A. Salishvhev, Acta Metall., 40, (1992), 581.

This work was performed under the auspices of the U.S. Department of Energy by Lawrence Livermore National Laboratory under contract No. W-7405-Eng-48.

CAPTIONS

Figure 3. Stress/strain behavior for constant strain-rate tests conducted at 1343 K.

Figure 4. Strain-enhanced growth of the β phase for constant strain-rate tests conducted at 1343 K.

Figure 3. Stress/strain behavior for constant strain-rate tests conducted at 1343 K.

Figure 4. Strain-enhanced growth of the β phase for constant strain-rate tests conducted at 1343 K.

Figure 5. Stress/strain behaviors for the longitudinal and transverse orientations. Tests were conducted at $\varepsilon=10^{-3}s^{-1}$ and 1343 K.

Figure 6. Fracture tip of a specimen tested in the longitudinal orientation at $\varepsilon=10^{-3}s^{-1}$ and 1343 K.

Figure 7. Grain size distributions for the b and (a+b) phases for the as-received and annealed microstructures. Grain sizes are expressed as a linear intercept value measured in the plane normal to the specimen thickness.

Figure 8. Stress/strain behaviors for the as-received and annealed conditions. Tests were conducted at $\varepsilon=10^{-3}s^{-1}$ and 1343 K.

Figure 9. Strain-rate sensitivites at 1343 K for the as-received and annealed microstructures.

Figure 9. Strain-rate sensitivites at 1343 K for the as-received and annealed microstructures.

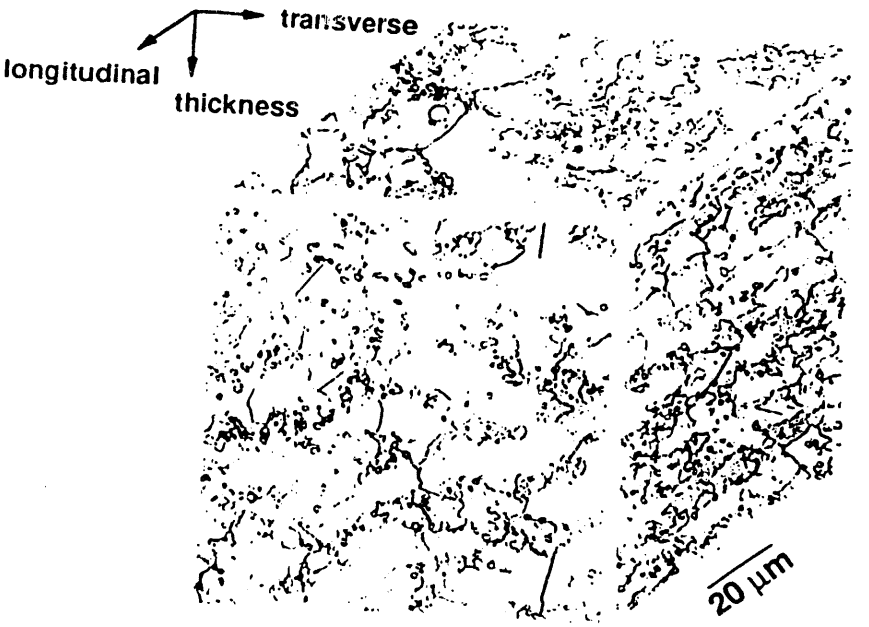


FIG 1

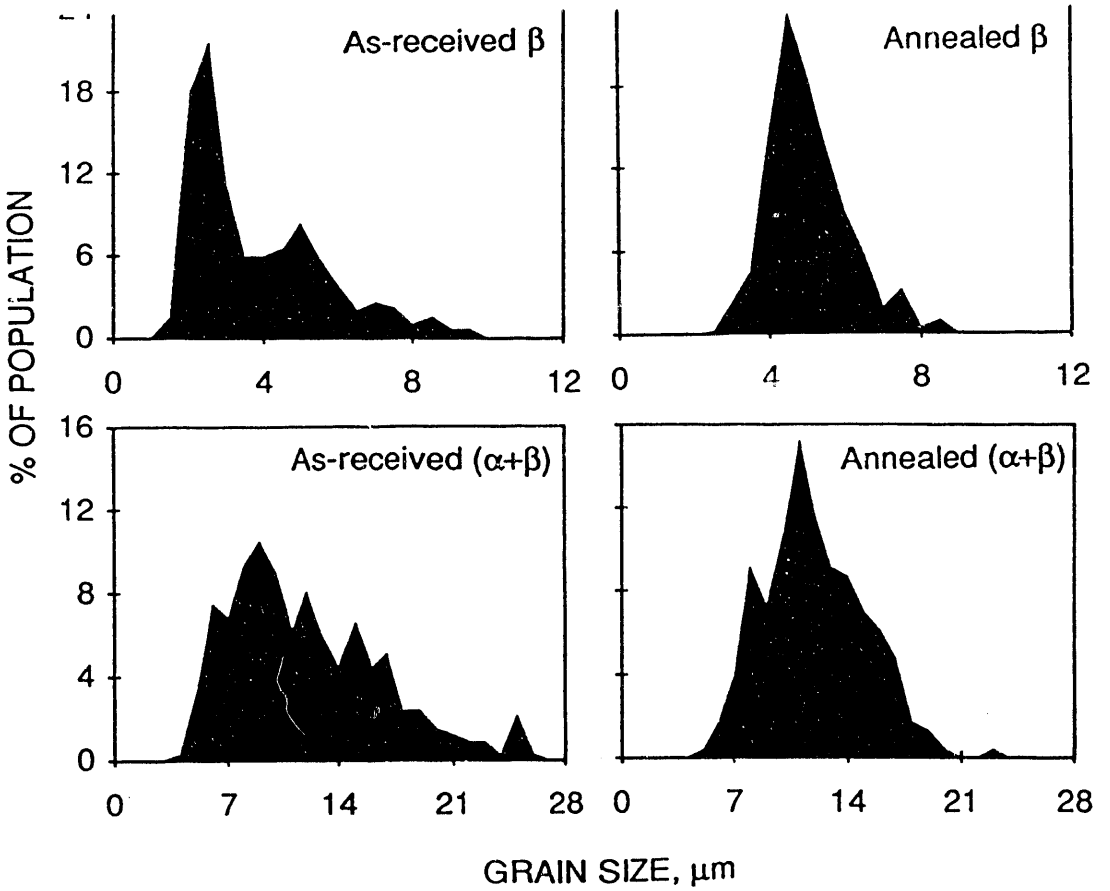
As-received β
Annealed β
As-received (α+β)
Annealed (α+β)
% OF POPULATION
GRAIN SIZE, μm
0
6
12
18
4
8
16
14
21
28
7

FIG 1→

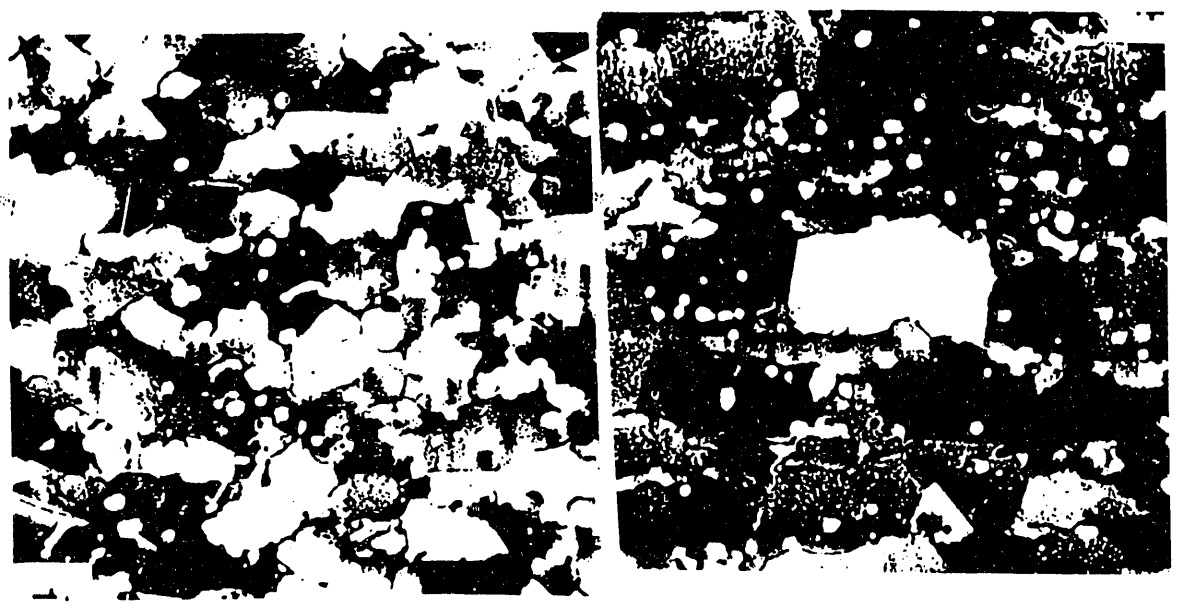

FIG 2

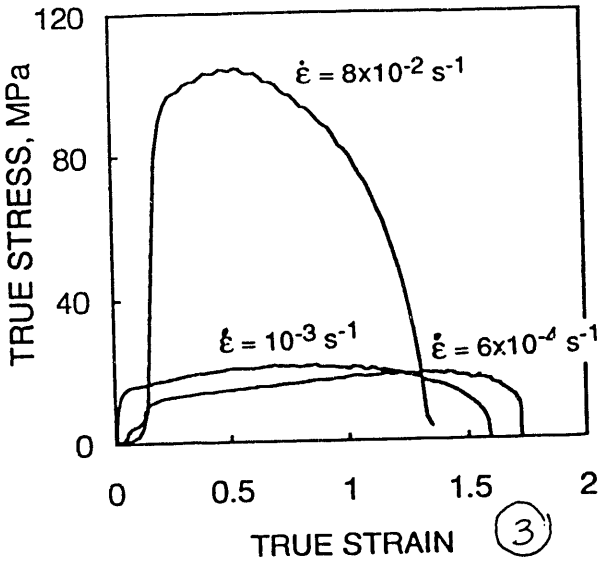
120
80
40
0
TRUE STRESS, MPa
$\dot{\varepsilon} = 8x10^{-2}\ s^{-1}$
$\dot{\varepsilon} = 10^{-3}\ s^{-1}$
$\dot{\varepsilon} = 6x10^{-4}\ s^{-1}$
0
0.5
1
1.5
2
TRUE STRAIN
3

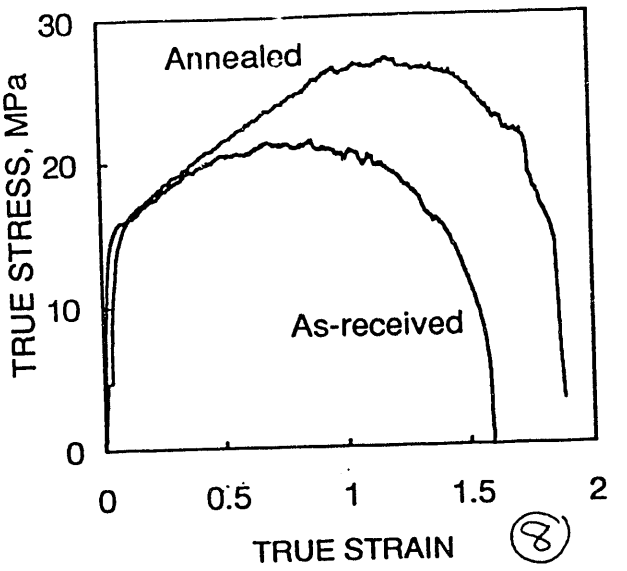
30
20
10
0
TRUE STRESS, MPa
Annealed
As-received
0
0.5
1
1.5
2
TRUE STRAIN
8

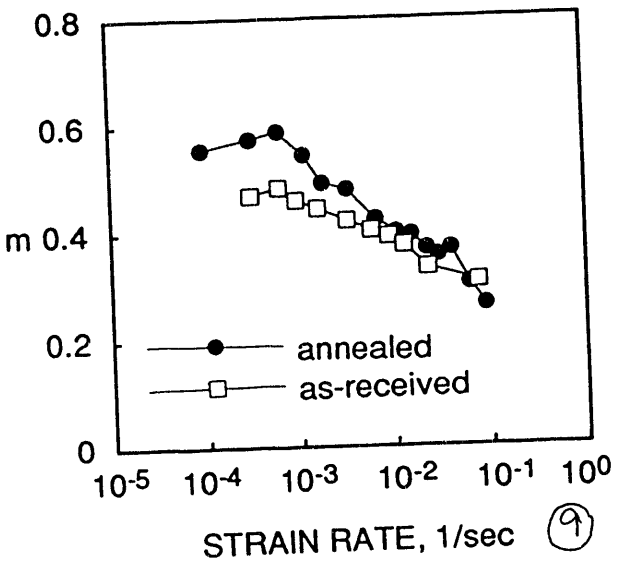
0.8
0.6
m 0.4
0.2
0
annealed
as-received
$10^{-5}$
$10^{-4}$
$10^{-3}$
$10^{-2}$
$10^{-1}$
$10^{0}$
STRAIN RATE, 1/sec
9

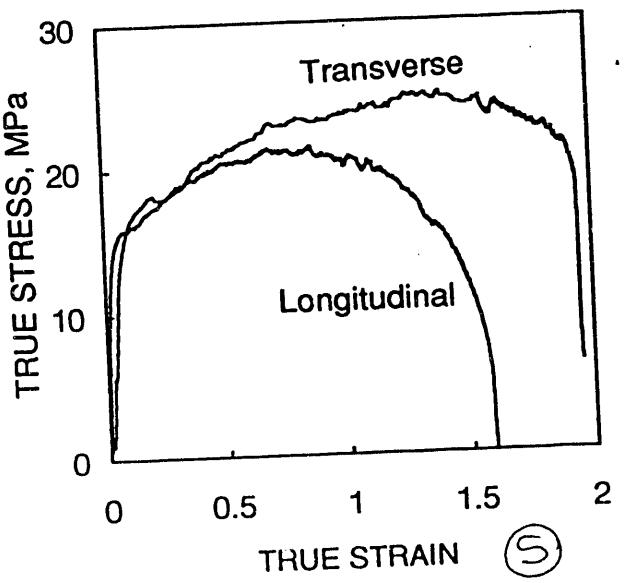
30
20
10
0
TRUE STRESS, MPa
Transverse
Longitudinal
0
0.5
1
1.5
2
TRUE STRAIN
5

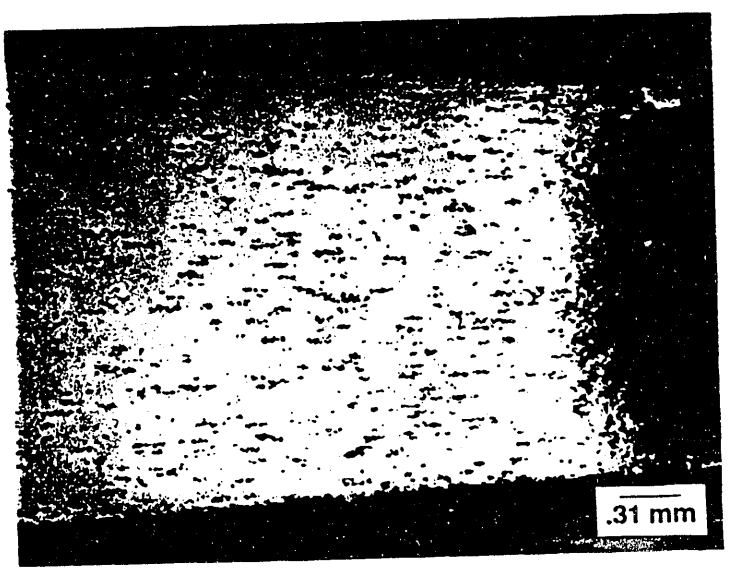
.31 mm

6

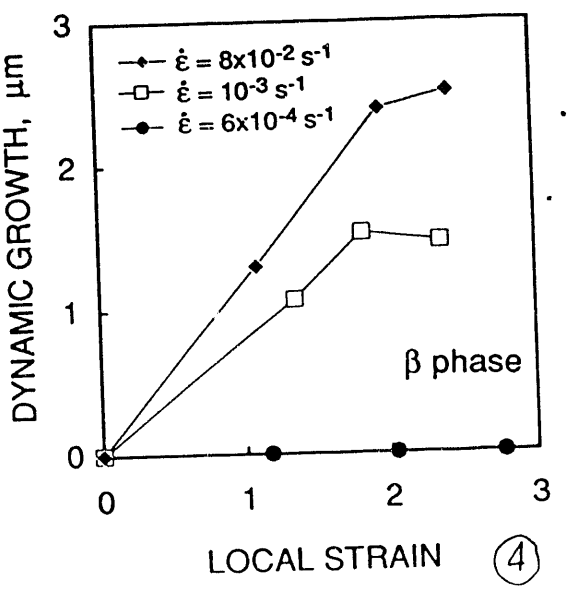
3
2
1
0
DYNAMIC GROWTH, μm
$\dot{\varepsilon} = 8x10^{-2}\ s^{-1}$
$\dot{\varepsilon} = 10^{-3}\ s^{-1}$
$\dot{\varepsilon} = 6x10^{-4}\ s^{-1}$
β phase
0
1
2
3
LOCAL STRAIN
4

DATE
FILMED
11/19/93
END